ACCOUNTS
of chemical research

Multistage Nanovectors: From Concept to Novel Imaging Contrast Agents and Therapeutics

BIANA GODIN,*,† ENNIO TASCIOTTI,† XUEWU LIU,†
RITA E. SERDA, AND MAURO FERRARI*

Department of Nanomedicine, The Methodist Hospital Research Institute, Houston, Texas, 77030, United States

RECEIVED ON MARCH 8, 2011

CONSPECTUS

Over the last few decades a great variety of nanotechnology based platforms have been synthesized and fabricated to improve the delivery of active compounds to a disease site. Nanoparticles currently used in the clinic, and the majority of nanotherapeutics/nanodiagnostics under investigation, accommodate single- or multiple- functionalities on the same entity. Because many heterogeneous biological barriers can prevent therapeutic and imaging agents from reaching their intended targets in sufficient concentrations, there is an emerging requirement to develop a multimodular nanoassembly, in which different components with individual specific functions act in a synergistic manner.

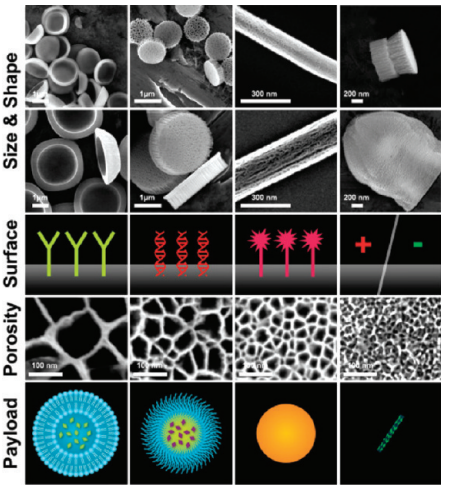

The multistage nanovectors (MSVs) were introduced in 2008 as the first system of this type. It comprises several nanocomponents or "stages", each of which is designed to negotiate one or more biological barriers. Stage 1 mesoporous silicon particles (S1MPs) were rationally designed and fabricated in a nonspherical geometry to enable superior blood margination and to increase cell surface adhesion. The main task of S1MPs is to efficiently transport nanoparticles that are loaded into their porous structure and to protect them during transport from the administration site to the disease lesion. Semiconductor fabrication techniques including photolithography and electrochemical etching allow for the exquisite control and precise reproducibility of S1MP physical characteristics such as geometry and porosity. Furthermore, S1MPs can be chemically modified with negatively/positively charged groups, PEG and other polymers, fluorescent probes, contrast agents, and biologically active targeting moieties including antibodies, peptides, aptamers, and phage.

The payload nanoparticles, termed stage 2 nanoparticles (S2NPs), can be any currently available nanoparticles such as liposomes, micelles, inorganic/metallic nanoparticles, dendrimers, and carbon structures, within the approximate size range of 5−100 nm in diameter. Depending upon the physicochemical features of the S1MP (geometry, porosity, and surface modifications), a variety of S2NPs or nanoparticle "cocktails" can be loaded and efficiently delivered to the disease site.

As demonstrated in the studies reviewed here, once the S2NPs are loaded into the S1MPs, a variety of novel properties emerge, which enable the design of new and improved imaging contrast agents and therapeutics. For example, the loading of the MRI Gd-based contrast agents onto hemispherical and discoidal S1MPs significantly increased the longitudal relaxivity (r1) to values of up to 50 times larger than those of clinically available gadolinium-based agents ($\sim$4 mM^{-1} s^{-1}/Gd^{3+} ion). Furthermore, administration of a single dose of MSVs loaded with neutral nanoliposomes containing small interfering RNA (siRNA) targeted against the EphA2 oncoprotein enabled sustained EphA2 gene silencing for at least 21 days. As a result, the tumor burden was reduced in an orthotopic mouse model of ovarian cancer.

We envision that the versatility of the MSV platform and its emerging properties will enable the creation of personalized solutions with broad clinical implications within and beyond the realm of cancer theranostics.

Introduction

The essential requirement in the administration of active agents is to achieve a favorable outcome in the treatment of a medical condition, minimizing detrimental adverse effects. However, the body encompasses a number of sequential, intrinsic defense mechanisms that efficiently prevent injected foreign agents such as chemicals, biopharmaceutics, and nanovectors from homing to their intended destinations.

Published on the Web 09/08/2011 www.pubs.acs.org/accounts
10.1021/ar200077p

In addition to general defense mechanisms, there are a number of disease-related heterogeneous barriers that adversely affect the biodistribution of untargeted and molecularly targeted therapeutics.[1,2] As a result, an extremely low fraction (<0.01%) of untargeted pharmaceuticals or specific antibodies has been shown to home to cancer lesions after intravenous administration.[1,3] The use of nanovectors as carriers for therapeutic and imaging contrast agents is based on the concurrent, projected advantages of drug localization at disease lesions, and the ability to circumvent the biological barriers encountered between the point of administration and the projected target.[4] Nanomedicine, a field at the intersection of nanotechnology, medicine, chemistry, physics, and biology, can take advantage of the recent developments in each of the above-mentioned research areas for the creation of platforms with superior drug carrier capabilities, selective responsiveness to the environment, unique contrast enhancement profiles, and improved accumulation at the disease site.

Nanovectors can historically be classified into three main subcategories, or generations.[2,5] First and second generations of nanovectors can be described as single-entity particles. First generation nanovectors, which made it to the clinic more than 15 years ago, passively home to the disease loci based on the permeability of tumor-associated neovasculature by a mechanism, known as enhanced permeation and retention (EPR).[6] Second-generation nanovectors offered new degrees of sophistication compared to their predecessors by employing additional complexities such as targeting moieties, remote activation, and environmentally sensitive components.[7−9] However, these improvements can be viewed simply as a progressive development of the first-generation vectors, which is conceptually unable to address the primary set of sequential biobarriers. As of today, none of the representatives of the second-generation subcategory have been granted FDA approval. The fundamental task of evading consecutive biobarriers has triggered a paradigm shift in the field of nanotherapeutics and, as a result, given rise to third-generation nanovectors, which decouple multiple tasks using separate nanocomponents, acting in a synergistic fashion. While a few platforms of third-generation nanocarriers are currently under investigation,[10,11] multistage nanovectors (MSVs), reviewed in this Account, are the emblematic system in this category.

The Multistage Concept

MSVs, introduced in 2008,[12] comprise several distinct nanoelements or "stages". Each stage is designed to negotiate one or several biobarriers from the site of administration to the target lesion. The nonspherical geometry of stage 1 mesoporous silicon particles (S1MPs) was selected in the process of rational mathematical design to enable superior blood margination and cell surface adhesion properties during the negotiation of biobarriers en route to the affected locus.[5,13] To yield a precise control of characteristics such as size, shape, and porosity, S1MPs are produced by semiconductor fabrication techniques: photolithography and electrochemical etching.[14] S1MPs were optimized to carry, protect, and distribute the second-stage nanoparticles (S2NPs) that are embedded within the porous structure and, once released at the vasculature of the lesion, can penetrate and diffuse into the tissue, delivering the therapeutic payload or enabling enhanced image contrast (Figure 1). The S1MP prevents direct exposure of the cargo to the body's surveillance system, inhibiting degradation of sensitive payloads and allowing avoidance of benign tissues. Following efficient margination in the bloodstream and attachment to the disease vasculature, MSVs release S2NPs containing any of the following: cytotoxic agents, contrast enhancing imaging agents, bioactives, or metal nanoparticles. In the case of metal S2NPs (e.g., gold, silver and iron oxide), the activation of the system can be triggered with an external energy source, such as radio frequency[15] or near-infrared[16] energy. Another possible mode of action includes targeting specific cell elements, such as macrophages and myofibroblasts, in the disease location to achieve preferential localization. The intracellular payload can then be released to destinations influenced by S1MP and S2NP surface chemistry. Similar principles can be applied for overcoming biobarriers specific to a variety of other conditions such as cardiovascular, infectious and neurological diseases.

Fabrication and Characterization of S1MPs

Nanoporous silicon (pSi) was chosen as the material for S1MP fabrication based on its biodegradability,[17−19] biocompatibility,[18,20] and versatile fabrication protocols allowing the control of shape, size, and porosity.[12] pSi-based nanostructured materials are widely explored for various biomedical applications including implantable devices,[21] drug delivery systems,[22−24] and tissue engineering scaffolds.[25] A series of combinatorial manufacturing protocols for S1MP fabrication were developed by integration of top-down electrochemical porosification with the industry standard silicon microfabrication process.[12,14,26] The silicon micromachining industry provides well-established techniques for

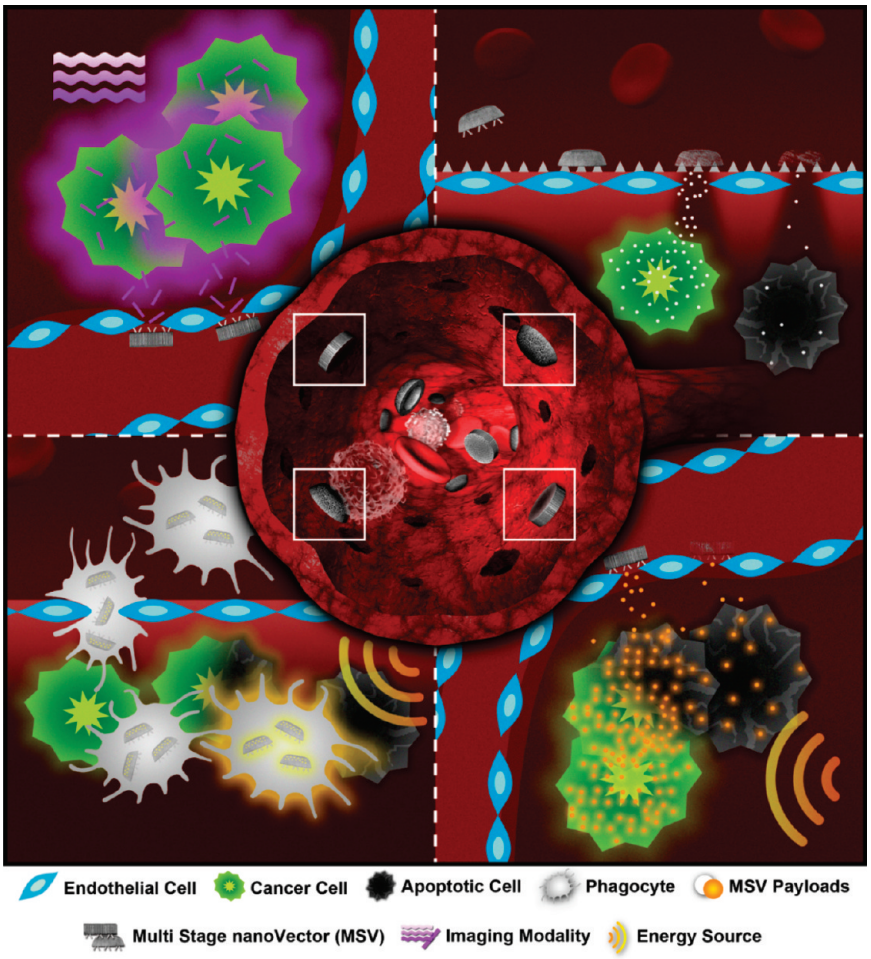

FIGURE 1. Schematic summary of possible MSV mechanisms of action. Central compartment: hemispherical or disk-shaped nanoporous silicon S1MPs are engineered to exhibit an enhanced ability to marginate within blood vessels and adhere to disease-associated endothelium. Once positioned at the disease site, the S1MP can (top right) release the drug/siRNA loaded S2NP to achieve the desired therapeutic effect, prior to complete biodegradation of the carrier particle; release an imaging agent (top left) or external energy activated S2NP (e.g., gold nanoparticles, nanoshells, bottom right). Another possible mechanism of action is cell based delivery of the MSVs into the disease loci followed by triggered release of the S1MP/S2NP from the cells (bottom left).

production and characterization, enabling scalability, precision, and reproducibility, important features for products intended for clinical translation.

The fabrication of S1MPs consists of two major steps: formation of nanoporous silicon by electrochemical etching and defining the particle pattern by photolithography. S1MP geometry is precisely controlled by photolithography, while the porous structure depends on the electrochemical etching parameters such as concentration of etching solution, doping, electrical current, and etching time (Figure 2).

The fabrication protocol of quasi-hemispherical S1MPs (Figure 2A), yielding monodisperse particles 900 nm to 3.2 μm in diameter, 30−65% porosity, and 3−55 nm pores, was described by Chiappini et al.[14] Briefly, starting with a silicon wafer coated with a dielectric silicon nitride (SiN) film, an array of particle patterns is first transferred to a dielectric layer by a photolithography process and reactive ion etch (RIE). A silicon etch is followed to define the trenches that nucleate S1MPs with different profiles.[14] A subsequent, two-step electrochemical etch process is applied to yield the S1MP of desired porosity, pore size, and thickness. A highly porous release layer is formed at the wafer−S1MP interface retaining S1MP on the substrate and allowing for differential chemical modifications of the two sides of S1MP if desired.

Discoidal vectors (Figure 2B) are fabricated by photolithographic patterning of a porous silicon film, a process that eliminates potential distortion effects introduced by nonuniform current distribution during electrochemical etch, simultaneously granting independent control of the porous structure. A novel sealing strategy to pattern pSi films using low pressure chemical vapor deposition of low temperature oxide (LTO) was implemented to overcome the problem of

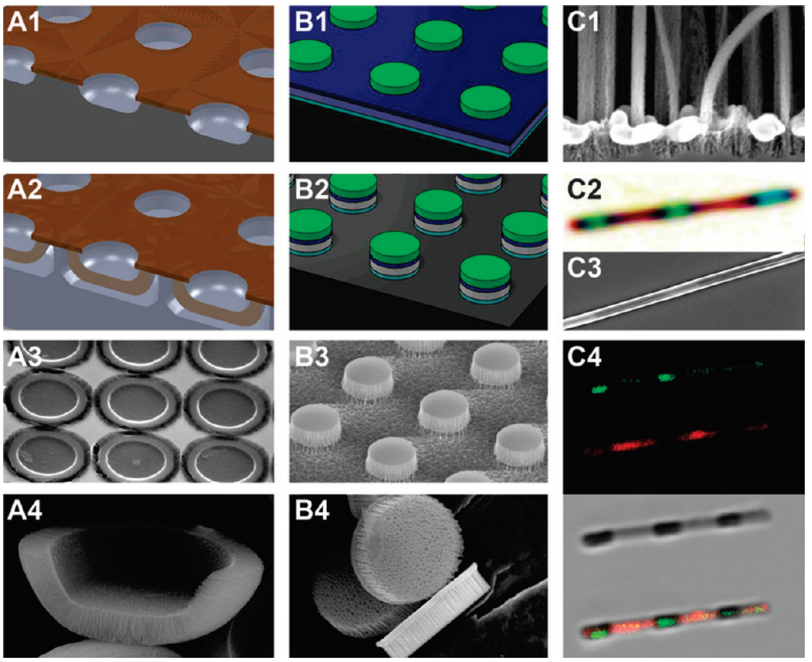

FIGURE 2. Fabrication of S1MP. (A1) Patterned SiN layer and trenches etched into silicon. (A2) Electrochemically etched S1MPs with release layer. (A3) S1MP array on wafer after removal of SiN. (A4) Cross-section of hemispherical S1MP. (B1) Photoresist pattern on LTO capped porous silicon film with release layer. (B2) Particle array on wafer after RIE. (B3) Discoidal S1MP array on wafer after LTO removal. (B4) Released discoidal S1MPs. (C1) Silver nanopattern etched into silicon forming porous silicon nanowires. (C2) Nanowire barcode under white light. (C3) SEM image of nanowire barcode. (C4) three-channel confocal microscopy images of nanowire barcode with green Q-dot loaded in small pore segment and red Q-dot in bigger pore segment.

photoresist adsorption within the pores. After electrochemical etch of double layered porous silicon films, the porous films is sealed by LTO, and an array of circles is patterned on the LTO film. A CF_4 RIE is then performed to etch through LTO and two layered porous silicon, producing monodisperse discoidal S1MPs with diameter as small as 400 nm and pore size ranging from 3 to 150 nm. The S1MP fabrication process is robust and well-characterized. Using 1000 nm diameter disks as an example, more than 2 billion S1MPs patterned on a 4″ wafer can be obtained. Our recent studies point toward the possibility for a multilayer fabrication method of discoidal particles, which should increase the production yield by tens times.

Porous silicon nanowires (Figure 2C) are fabricated by metal assisted electroless etch in a solution of HF and H_2O_2 following deposition of Ag nanopatterns.[27] pSi barcode nanowires were fabricated with multiple segments of different porosities by tuning the concentration of hydrogen peroxide during metal assisted etch, and multicolor reflection and photoluminescence from a single barcode nanowire were demonstrated. The morphology of nanowires is a function of metal employed, H_2O_2 concentration, ethanol concentration, and silicon resistivity, while the geometry and density of the nanowires can be controlled by means of nanoscale lithography. These novel structures can be used as a drug delivery platform, as demonstrated through a segment-specific loading of quantum dots (QDs) of two different sizes.

Effect Physicochemical Characteristics on S2NP Loading and Release

The versatility in the design parameters of S1MPs enables them to serve as carriers for a wide spectrum of therapeutic and diagnostic S2NPs. At the same time, MSVs can be optimized to release their cargo in a controlled fashion as summarized in Figure 3. Loading of the porous silicon matrix occurs by the incipient wetness method, with retention based on electrostatic interactions.[12,23,28] The pore size and surface charge of the S1MP can be tailored and optimized for the loading and release of virtually any type of S2NP. The knowledge of the S2NP composition, surface charge, size, and concentration guides the choice of the physical and chemical features of the MSV. In general, four critical factors determine the loading efficiency of S2NPs into S1MPs as well as the way they will be retained and eventually released: (1) physicochemical characteristics of S2NPs; (2) surface potential of S1MPs; (3) pore size, morphology, and density of S1MPs; and (4) conditions in which the degradation/release occurs. The size of the pores obviously

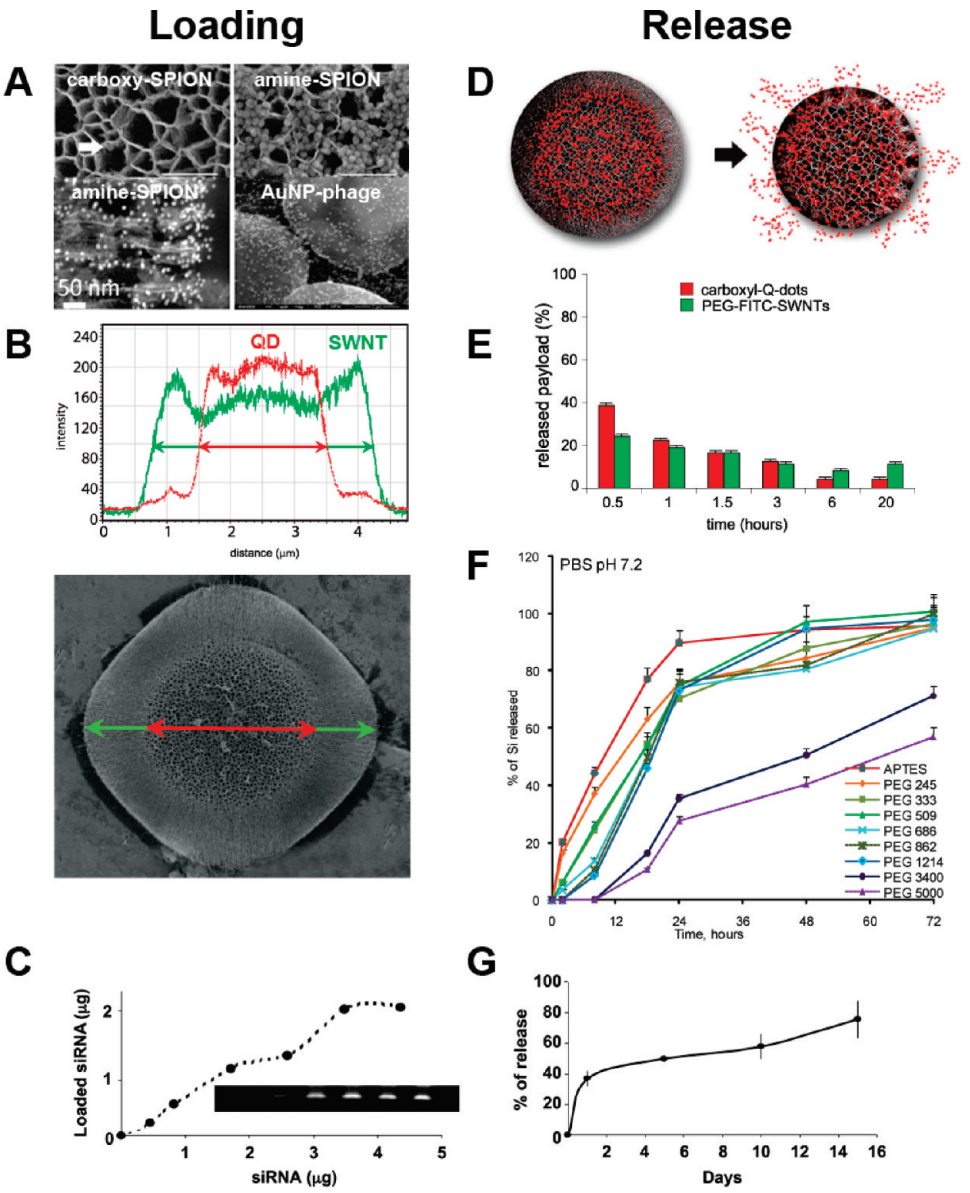

FIGURE 3. Loading and release of S2NPs to/from S1MPs. (A) Loading of negatively and positively charged SPIONs into discoidal oxidized (−) S1MPs and the association of gold nanoparticles/phage displaying targeting peptide assemblies on top of hemispherical S1MP; (B) coloading and (E) corelease of QDs and PEGylated single-wall carbon nanotubes (SWNTs) to/from a hemispherical particle with differential porosities; (D) schematic presentation of the payload release from S1MP in the process of degradation; (F) tuning degradation kinetics of the hemispherical 3.2 μm S1MP through covalent conjugation of PEG possessing various molecular weights; loading (C) and release (G) of siRNA containing liposome (DOPC) into the hemispherical 1.6 μm S1MP. Parts of this Figure are reproduced with permission from refs 12, 18, 23, and 28. Copyright 2008, 2010 Nature Publishing Group, John Wiley and Sons, and American Association of Cancer Research.

governs the nature of S2NPs that can be loaded into S1MPs. S2NPs with a nominal diameter larger than pore size will remain loosely associated with the pSi surface based on electrostatic interactions. By modifying the pore size and S2NP diameter, various payloads can be associated with the same S1MP as shown in Figure 3 for carbon nanotubes (SWNTs) with $d = 2-3$ nm and 50 nm length and QD ($d = 15$ nm).[12] When S2NPs possess diameters smaller than the pore size in S1MP, the loading process is governed by capillary forces acting on a liquid suspension flowing into a porous matrix. The retention of the loaded cargo and its stability in circulation, dependent on the interaction between the payload and the carrier, is governed by electrostatic interactions. S2NPs with a similar charge to that of the S1MPs are partially or completely repelled from the pores. Oxidized S1MPs with negative net surface potential due to the presence of hydroxyl units can be efficiently loaded with S2NPs of a near neutral or positive surface potential,

but fail to load S2NPs with a negative surface charge (Figure 3A).[28,29] As an example, a scanning electron microscopy (SEM) image shows only a single carboxylated superparamagnetic iron oxide nanoparticle (carboxy-SPION). Conversely, an abundance of amine-modified SPIONs (amine-SPION) are found within the porous matrix throughout the length of the pores when loaded under the same conditions. In order to accommodate negative nanoparticles within the pores, S1MPs can be modified with 3-aminopropyltriethoxysilane (APTES).

Theoretically, the pore volume of each 1000 nm $\times$ 400 nm GP particle is about 0.2 μm^3, in which up to 3.8 $\times$ 10^5 10 nm S2NPs can be loaded. Empirically, loading of 0.3 pg of 10 nm SPIONs per S1MP particle was detected, corresponding to $\sim 1 \times 10^5$ SPIONs.

The release kinetics of the S2NPs can be linked to the degradation of the S1MP and can be adjusted by controlling their porosity or pore distribution. Alternatively, the particles can be embedded into, conjugated to, or coated with polymer shells that delay the release of the payload. Conjugation of polyethylene glycols (PEGs) of various molecular weights to the surface of S1MP had a significant effect on particle degradation kinetics. Quantitative analysis (Figure 3F) and SEM visualization have shown that degradation of S1MP can be considerably delayed when high MW PEGs are covalently attached to the surface.[18]

Surface Chemistry Prescribed Logic-Embedded Intracellular Trafficking

A unique feature of multistage multiparticle delivery systems is the ability of a single delivery vehicle to be "intracellularly partitioned" into separate regions and trafficked to distinct cellular locations. Through fine control of S1MP and S2NP surface chemistry, various stages of MSVs can concurrently or consecutively be delivered to intracellular locations for multiple autonomous or synergistic effects (Figure 4). Furthermore, the cargo can comprise a combination of imaging and therapeutic agents, creating a theranostic system for real time monitoring of intracellular drug delivery with concomitant therapeutic effect.

To evaluate the impact of the surface chemistry on intracellular release and trafficking of S2NPs, SPIONs with different surface characteristics were loaded into discoidal S1MPs and delivered to mouse macrophages.[28] Following the internalization, within the endosome, SPIONs were shown to dissociate from the S1MPs. Following a surface modification of SPIONs with a PEGylated amine, endosomal sorting of particles led to the formation of vesicular regions rich in S2NPs.[28] These SPION-rich regions are believed to bud off of the endosome, creating novel vesicles which were seen both intracellularly and in association with the outer plasma membrane, indicating vesicular release from the cell (Figure 4B, left). The ability of cells to communicate with other cells in a contact-independent manner through secretion and uptake of vesicles containing both cellular and nanoparticle-delivered signals, as well as cellular protein, RNA, and lipid, allows for rapid signal propagation, expanding the impact of the therapeutic agent to the entire lesion microenvironment. Alternatively, when SPION S2NPs were modified with chitosan, they escaped from the endosome and entered the cytosol (Figure 4B, right). The data support the notion that nanovector surface chemistry can govern delivery to intracellular destinations and intracellular communication, which in an MSV system can be programmed in a logic-embedded fashion.

The biocompatibility of MSVs was tested and confirmed in a number of in vitro and in vivo studies. S1MP were shown to degrade in physiological environments in vitro and in vivo.[18,23] In vitro studies in endothelial cells and macrophages have demonstrated that, following the interaction with MSVs, the cells do not produce inflammatory cytokines (33 cytokines were tested), and exhibit normal cell cycle.[18,30] Cellular proliferation, cell cycle, and apoptosis are all unaltered by the presence of the internalized microparticles.[30] Mitosis of cells, with as many 30 microparticles, supported normal partitioning of endosomes between daughter cells, despite the presence of the microparticles within the endosomal vesicles (Figure 4C). In in vivo studies examining the effect of MSV acute and subchronic administration in healthy mice, no release of biochemical markers and plasma cytokines was observed.[18]

MSVs as Advanced Imaging Agents

Magnetic resonance imaging (MRI) is currently one of the most powerful noninvasive diagnostic imaging techniques, and early diagnosis, treatment, and prognosis of numerous conditions depend on the ability to provide greater MRI resolution. Relaxivity (ri), which expresses the ability of a paramagnetic material to perform as an MRI contrast agent, can be described as the change in the relaxation rate (1/Ti) of water protons normalized to the concentration of the contrast agent (CA). The majority of clinically used MRI CAs are based on Gd^{3+} ions which are highly toxic in a free form and thus have to be chelated. Though chelation minimizes the toxicity of Gd^{3+} ions, it also reduces the number of coordination sites, resulting in low relaxivities of less than 4 mM^{-1} s^{-1}

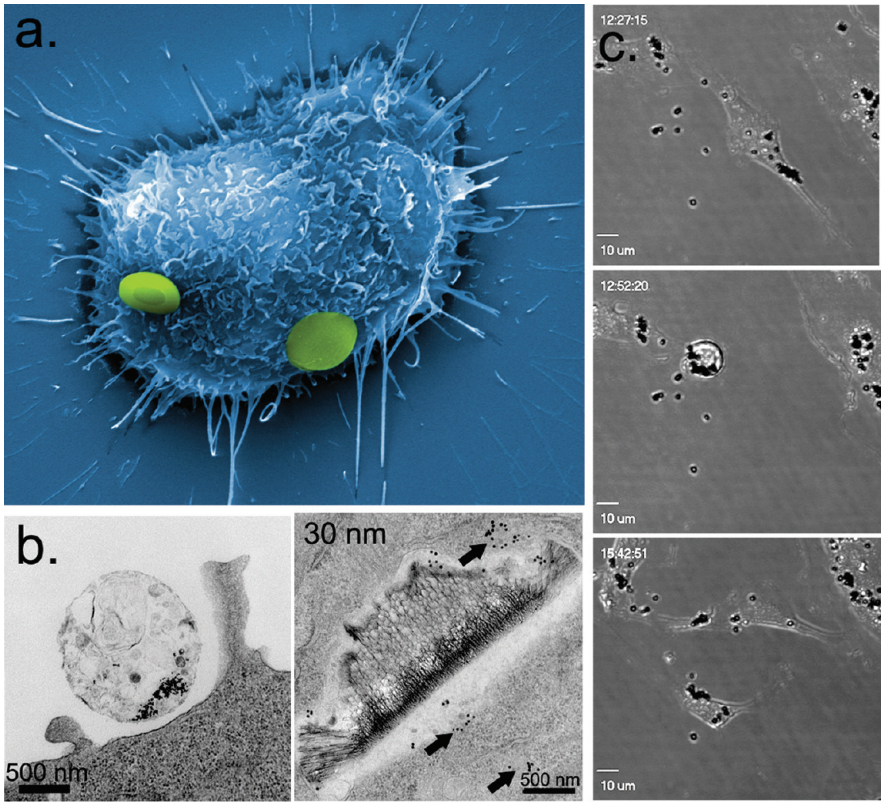

FIGURE 4. Intracellular delivery of MSVs. (A) SE micrograph of early stage S1MP phagocytosis in an endothelial cell. (B) TE micrographs showing a secreted SPION-loaded vesicle (left) and an internalized MSV with dual cell localization (right; endosome and cytosol).[28] (C) Live confocal images of endothelial mitosis in the presence of internalized S1MPs, showing how S1MPs in the parent cell are split between the two daughter cells. Parts of this Figure are reproduced with permission from ref 28. Copyright 2010 John Wiley and Sons.

at 1.41 T. Using the MSV approach, a new category of MRI contrast enhancing agents was designed through loading Gd-based CAs, such as a clinically used chelate (Magnevist, MAG) and Gd^{3+} loaded carbon nanoparticles (carbon nanotubes, GDNT; and fullerenes, GF), into the nanoporous structure of discoidal (D) or hemispherical (HS) S1MPs (Figure 5A).[26] The resulting MSV constructs showed a significant boost in longitudinal relaxivity resulting in up to 40 times higher values than clinically used MAG. The proposed mechanism of the prominent enhancement in the MRI contrast is based on the geometrical confinement of Gd CAs within the porous silicon S1MPs, which affects the paramagnetic behavior of the Gd^{3+} ions by enhancing interactions between neighboring CAs through reducing the mobility of water molecules and the potential of CAs to rotate.[26]

SPIONs were another MRI contrast agent tested as S2NPs. SPIONs have a greater impact on transverse, spin−spin relaxation (T2, decrease $x-y$ component), leading to areas of negative contrast. Transverse relaxations due to susceptibility (T_2*) measured using a multigradient echo sequence in the presence or absence of SPIONs have shown that loading of S1MPs with SPIONs led to shorter relaxation times, in a SPION concentration-dependent manner (Figure 5B).[28] The differences in signal intensities were more dramatic at lower echo times in gradient-echo images (Figure 5B, the four images below). The ability to load an abundance of SPIONs within a single silicon particle supports delivery of a large contrast agent payload to a single target, creating a powerful contrast agent with the ability for single cell imaging and targeted delivery.

The surface of the S1MP provides a suitable platform for covalent conjugation and electrostatic attachment of a vast spectrum of dyes, fluorophores, fluorescent tags, radioactive molecules, and other imaging contrast agents. Systems such as phage displaying targeting peptides/gold nanoparticles networks (nanoshuttles) can be easily attached to the surface of the S1MP based on electrostatic interactions producing multifunctional nanoassemblies (Figure 3A). Established protocols for silane chemistry enable the use of several commercially available bioconjugation kits for easy covalent functionalization of the S1MP surface. This allows for incorporation of imaging components, such as near-infrared (NIR) dye, single photon emission computed tomography agent,

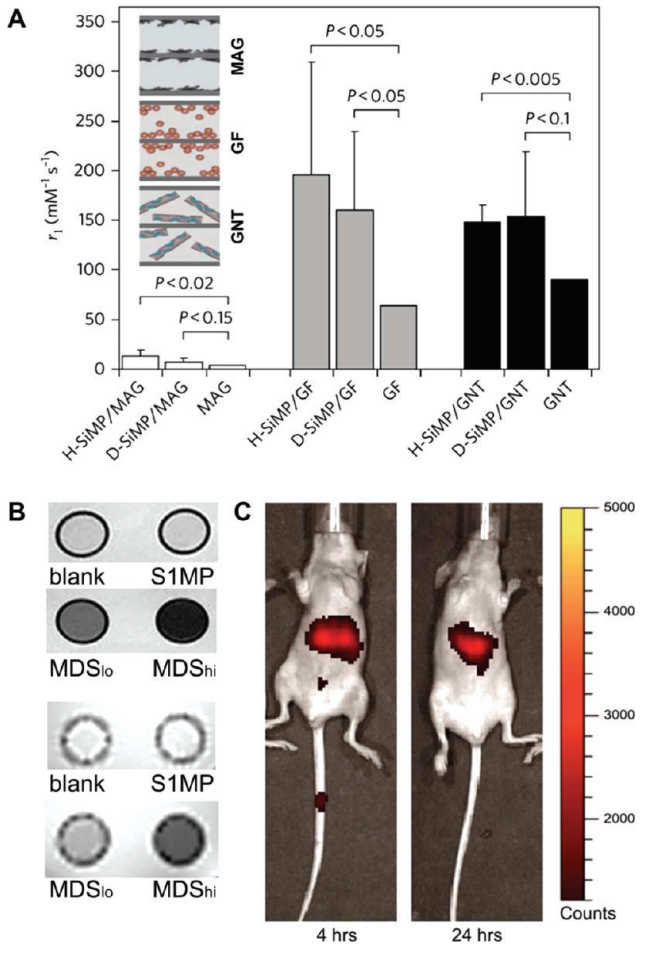

FIGURE 5. MSVs as advanced imaging agents. (A) Longitudinal relaxivity, r_1, of the MSV based new MRI nanoconstructs measured by a benchtop relaxometer as compared with the corresponding Gd-based CAs.[26] (B) Axial spin- (top) and gradient- (bottom) echo magnetic resonance images of NMR tubes containing PBS (blank), S1MPs, and MSVs loaded with SPIONs (MDS_{lo} and MDS_{hi}).[28] (C) In vivo NIR imaging following intravenous administration of 3.2 μm hemispherical S1MPs tagged with Dylight 750.[31] Parts of this Figure are reproduced with permission from refs 26, 28, and 31. Copyright 2010, 2011 Nature Publishing Group, John Wiley and Sons, and Decker Publishing.

and positron emission tomography agent, onto the S1MP surface, while still keeping the pores available for loading S2NPs with additional synergistic functionalities. NIR represents another technique that is currently being used in clinic, since the intrinsic absorption from tissue and molecules in this spectral region is minimal. Through conjugation of an NIR probe to the surface of S1MPs, the biodistribution of the nanovectors in healthy mice was successfully tracked and the accumulation of the NIR-S1MPs in the different organs was quantified based on image analysis (Figure 5C).[31] The biodistribution observed through NIR imaging for up to 72 h from the time of administration was further confirmed by a quantitative analysis of silicon in the different organs by inductive coupled plasma atomic emission spectroscopy (ICP-AES). While direct conjugation of imaging agents to the surface of S1MP provided a method to monitor MSV distribution, this strategy is dependent on the stable conjugation of molecules to the S1MP surface. Thus, in the time course of events, when the S1MP undergoes degradation, covalently bound molecules gradually detach from the surface, making in vivo imaging less reliable and accurate. On the other hand, imaging agents are expected to be efficiently cleared after fulfillment of their function. Flow dynamics and tumor accumulation of fluorescently labeled MSVs of various geometries is currently being investigated using ICP and intravital microscopy. Recent biodistribution data in mice show that for untargeted disk-shaped S1MPs up to 10%/g tissue of the injected dose homes to tumors (Godin et al. and VandeVen et al., unpublished data). When spherical particles are considered, no more than 2% of the injected dose/g tissue is accumulated in the tumor (Godin et al., unpublished data).

MSVs as Novel Therapeutic Agents

One of the first agents tested with MSVs belongs to the class of small interfering RNA (siRNA) therapeutics, which are double-stranded RNAs able to specifically suppress the activity of a gene.[32] siRNAs were discovered a decade ago by Fire et al.,[33] opening new therapeutic avenues via the selective downregulation of pathological proteins. The results of a recent phase I trial on a patient with refractory solid tumor demonstrated the first clinical proof of concept that gene silencing can be achieved following a systemic administration of siRNA.[34] However, clinical translation of this promising concept is significantly hampered by several limitations due to some of the following aforementioned biobarriers: extensive and prompt siRNA degradation by nucleases in the bloodstream and the inability of this hydrophilic substance to efficiently cross cell membranes to reach the target site.

Liposomes were investigated as a delivery system for siRNA therapeutics which can protect them from degradation and inhibit harmful nonspecific binding to normal tissues. In vitro and in vivo studies have demonstrated some improvement of siRNA delivery to melanoma, lung cancer, breast cancer, and ovarian cancer when liposomal carriers were used.[35,36] The efficacy of MSVs loaded with neutral dioleoyl phosphatidylcholine (DOPC) nanoliposomes containing EphA2-specific siRNA was evaluated in two independent orthotopic mouse models of ovarian cancer.[23] EphA2 is an oncoprotein overexpressed in most malignancies including ovarian tumors. After a single treatment with EphA2-targeted MSVs and without concurrent chemotherapy,

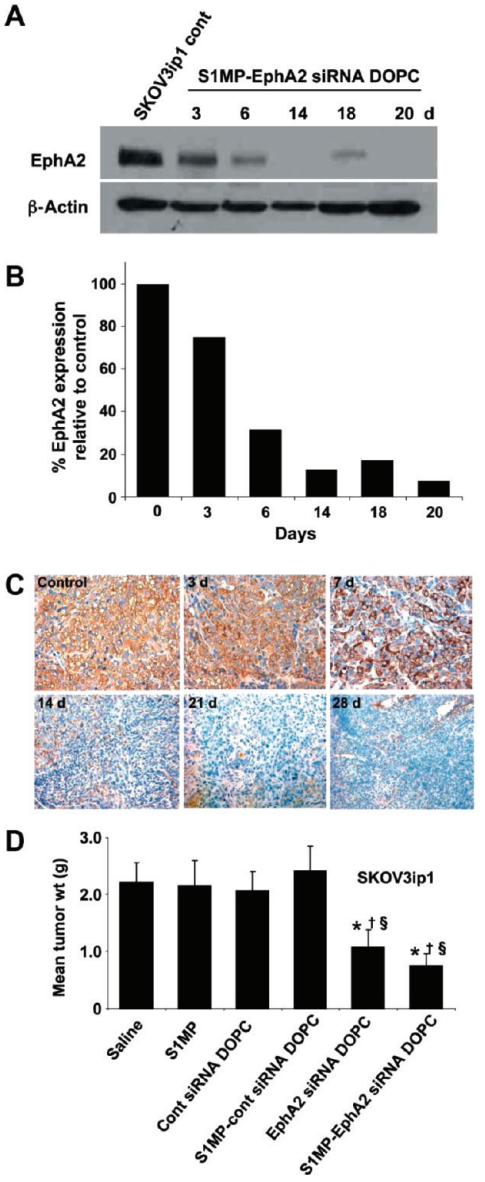

FIGURE 6. Systemic delivery of siRNA-DOPC using S1MPs results in long-lasting in vivo gene silencing. Mice with SKOV3ip1 orthotopic ovarian tumors were injected with S1MP-EphA2-siRNA-DOPC or left nontreated. (A) Western blot to measuring EphA2 expression levels at predetermined time-points. (B) densitometric analysis of normalized EphA2 expression by β-actin; (C) immunohistochemical analysis of EphA2 expression in the SKOV1ip3 tumor; (D) therapeutic efficacy of sustained EphA2-siRNA-DOPC delivery by S1MPs in SKOV3ip1 bearing mice. Treatment groups ($n = 10$): saline, S1MP, nonsilencing control siRNA-DOPC, S1MP-nonsilencing control-siRNA-DOPC, EphA2-siRNA-DOPC, and S1MP-EphA2-siRNA-DOPC (MSV). SiRNA-DOPC was intravenously injected biweekly at a dose of 5 μg of siRNA. S1MP-EphA2-siRNA-DOPC was injected as a single administration in 3 weeks at a dose of 15 μg of siRNA. Reproduced from ref 23 with permission from AACR.

gene silencing and decrease in tumor burden, evaluated through cell proliferation (K_i-67) and angiogenesis (CD31), were observed (Figure 6). To achieve a similar effect with siRNA-DOPC, twice higher dose administered in six aliquots (twice a week for 3 weeks) was required. The mechanism of the efficient and sustained liposomal siRNA delivery was likely to rely on surface modification, tissue distribution, and slow biodegradation of the S1MPs. S1MPs not only served as storage for liposomal siRNA but also shielded siRNA oligos from degradation by enzymes inside the body. This novel approach opens new avenues in personalization of siRNA therapeutics through controlled delivery of synergistic payloads in a time-controllable fashion.

Conclusions and Perspectives

Personalization of treatment is the focus of research worldwide, with overwhelming bias toward personalization by way of molecular target recognition. The progressive evolution in the field of nanotechnology can provide additional and required dimensions to the personalization of treatment by integrating chemistry, mathematics, physics, and engineering science to synthetize by-design therapeutics, sensitive and lesion-specific imaging agents, and responsive theranostic vectors.

Multistage nanovectors, described in this Account, were rationally designed as the first modular system that can systematically address sequential biobarriers in a controllable/chronological fashion. One of the key features of the MSVs is the capacity to incorporate and take advantage of a variety of existing, novel, or clinically used, therapeutic and imaging vectors from a "nano-toolbox", while enabling synergistic application of these nanotechnologies to form a higher generation nanosystem. Some examples of the advantageous loading of S2NPs in S1MPs to produce MSVs are summarized in Table 1 of the Supporting Information. The versatility of the MSV platform allows for a multiplicity of applications. Moreover, upon loading of the S2NPs into S1MPs, a variety of new properties emerge, enabling design of new generations of imaging contrast agents and therapeutics.

BIOGRAPHICAL INFORMATION

Dr. Biana Godin (Vilentchouk) is an Assistant Member of The Methodist Hospital Research Institute and an Adjunct Professor at the University of Texas Graduate School of Biomedical Sciences at Houston. She earned her Ph.D. in Pharmaceutical Sciences from the Hebrew University of Jerusalem in 2006. In 2007 she was recruited as a Postdoctoral trainee to the Nanomedicine research team of Dr. Mauro Ferrari at the University of Texas Health Sciences Center. She has published more than 50 peer-reviewed papers, reviews, and book chapters. Her work published in top journals,

including *Nature Nanotechnology*, *Journal of Controlled Release*, and *Cancer Research*, and provided insightful understanding of the interactions of multistage nanovectors with immune cells, effect of geometry and targeting moieties on MSV biodistribution, and evaluation of MSV systems imaging potential.

Dr. Ennio Tasciotti is an Associate member of The Methodist Hospital Research Institute in the Department of Nanomedicine and serves as Interim Co-Chair of Regenerative Medicine. He is also the Scientific Director of the Spine Advanced Technology Laboratory and is an Adjunct Professor at the University of Texas Graduate School of Biomedical Sciences at Houston. Dr. Tasciotti was trained in Molecular Biology at Scuola Normale Superiore of Pisa and received his Ph.D. in Molecular Medicine at the International Center for Genetic Engineering and Biotechnology. He was an inventor of the multistage nanovectors, and his research focuses on unconventional, biology inspired, delivery systems.

Dr. Xuewu Liu is an Associate Member of The Methodist Hospital Research Institute and an Adjoint Professor in Department of Biomedical Engineering at University of Texas at Austin. He received his Ph.D. in Physics from Kent State University in 2002. Dr. Liu started nanomedicine research in Dr. Ferrari's laboratory at Ohio State University in 2003, and in 2006 became an Assistant Professor at University of Texas Health Science Center at Houston. He directs the research and development of silicon based nanomaterials and nanodevices. The nanomedicine platforms he developed include nanoporous silicon particles, nanowire barcodes, nanochannel drug delivery implants, and nanoporous proteomic chips.

Dr. Rita Serda is an Assistant Member and an interim cochair of Nanomedicine at The Methodist Hospital Research Institute, Houston, Texas. She is Director of the Scanning Electron Microscopy Core and the Faculty Director of the Methodist Academy. Dr. Serda has published 27 peer-reviewed journal articles, and her work has been featured on the cover of 5 peer-reviewed journals. She has 6 published/forthcoming book chapters and is currently editing her first book.

Dr. Mauro Ferrari serves as President and CEO of The Methodist Hospital Research Institute, where he holds the Ernest Cockrell Jr. Distinguished Endowed Chair. He is also Professor of Internal Medicine at the Weill Cornell Medical College and holds Adjunct Professor positions with UT M.D. Anderson Cancer Center, Rice University, and UT Austin. Dr. Ferrari is also a President of The Alliance for NanoHealth in Houston. Dr. Ferrari is a founder of biomedical nano/microtechnology, especially in their applications to drug delivery, cell transplantation, implantable bioreactors, and other innovative therapeutic modalities. He has published more than 200 peer-reviewed journal articles and 6 books. He is the inventor of more than 30 issued patents, with about 30 more pending in the United States and internationally. His contributions have been recognized by a variety of prestigious international accolades.

Mathew Landry is greatly acknowledged for the graphical design. The authors acknowledge financial support from the following sources: NIH U54CA143837 (CTO, PSOC), NIH 1U54CA151668-01 (TCCN, CCNE), DODW81XWH-09-1-0212, and DODW81XWH-07-2-0101.

Supporting Information. Table showing examples of advantageous loading of S2NP in S1MP to produce MSVs. This material is available free of charge via the Internet at http://pubs.acs.org.

FOOTNOTES

*To whom correspondence should be addressed. (B.G.) Mailing address: The Methodist Hospital Research Institute, 6670 Bertner St., R7-122, Houston, TX 77030. Telephone: 713-4417329 (office), 713-4059076 (cell). E-mail: BGodin@tmhs.org. (M.F.) Mailing address: The Methodist Hospital Research Institute, 6670 Bertner St., M.S. R2-216, Houston, TX 77030. Web: www.tmhri.org. Telephone 713-441 8439. E-mail: MFerrari@tmhs.org.
†Equal contribution.

REFERENCES

1 Jain, R. K. Physiological barriers to delivery of monoclonal antibodies and other macromolecules in tumors. *Cancer Res.* **1990**, *50*, 814s–819s.
2 Ferrari, M. Cancer nanotechnology: opportunities and challenges. *Nat. Rev. Cancer* **2005**, *5*, 161–171.
3 Jain, R. K. Transport of molecules, particles, and cells in solid tumors. *Annu. Rev. Biomed. Eng.* **1999**, *1*, 241–263.
4 Jain, R. K.; Stylianopoulos, T. Delivering nanomedicine to solid tumors. *Nat. Rev. Clin. Oncol.* **2010**, *7*, 653–664.
5 Godin, B.; Driessen, W. H.; Proneth, B.; Lee, S. Y.; Srinivasan, S.; Rumbaut, R.; Arap, W.; Pasqualini, R.; Ferrari, M.; Decuzzi, P. An integrated approach for the rational design of nanovectors for biomedical imaging and therapy. *Adv. Genet.* **2010**, *69*, 31–64.
6 Maeda, H.; Matsumura, Y. EPR effect based drug design and clinical outlook for enhanced cancer chemotherapy. *Adv. Drug Delivery Rev.* **2010**, *63*, 129–130.
7 Torchilin, V. P. Recent advances with liposomes as pharmaceutical carriers. *Nat. Rev. Drug Discovery* **2005**, *4*, 145–160.
8 Debbage, P. Targeted Drugs and Nanomedicine: Present and Future. *Curr. Pharm. Design* **2009**, *15*, 153–172.
9 Bardhan, R.; Chen, W.; Perez-Torres, C.; Bartels, M.; Huschka, R. M.; Zhao, L. L.; Morosan, E.; Pautler, R. G.; Joshi, A.; Halas, N. J. Nanoshells with Targeted Simultaneous Enhancement of Magnetic and Optical Imaging and Photothermal Therapeutic Response. *Adv. Funct. Mater.* **2009**, *19*, 3901–3909.
10 Sengupta, S.; Eavarone, D.; Capila, I.; Zhao, G.; Watson, N.; Kiziltepe, T.; Sasisekharan, R. Temporal targeting of tumour cells and neovasculature with a nanoscale delivery system. *Nature* **2005**, *436*, 568–572.
11 Wong, C.; Stylianopoulos, T.; Cui, J.; Martin, J.; Chauhan, V. P.; Jiang, W.; Popovic, Z.; Jain, R. K.; Bawendi, M. G.; Fukumura, D. Multistage nanoparticle delivery system for deep penetration into tumor tissue. *Proc. Natl. Acad. Sci. U.S.A.* **2011**, *108*, 2426–2431.
12 Tasciotti, E.; Liu, X.; Bhavane, R.; Plant, K.; Leonard, A. D.; Price, B. K.; Cheng, M. M.; Decuzzi, P.; Tour, J. M.; Robertson, F.; Ferrari, M. Mesoporous silicon particles as a multistage delivery system for imaging and therapeutic applications. *Nat. Nanotechnol.* **2008**, *3*, 151–157.
13 Decuzzi, P.; Ferrari, M. Design maps for nanoparticles targeting the diseased microvasculature. *Biomaterials* **2008**, *29*, 377–384.
14 Chiappini, C.; Tasciotti, E.; Fakhoury, J. R.; Fine, D.; Pullan, L.; Wang, Y. C.; Fu, L.; Liu, X.; Ferrari, M. Tailored Porous Silicon Microparticles: Fabrication and Properties. *ChemPhysChem* **2010**, *11*, 1029–1035.
15 Glazer, E. S.; Zhu, C.; Massey, K. L.; Thompson, C. S.; Kaluarachchi, W. D.; Hamir, A. N.; Curley, S. A. Noninvasive radiofrequency field destruction of pancreatic adenocarcinoma xenografts treated with targeted gold nanoparticles. *Clin. Cancer Res.* **2010**, *16*, 5712–5721.
16 Loo, C.; Lin, A.; Hirsch, L.; Lee, M. H.; Barton, J.; Halas, N.; West, J.; Drezek, R. Nanoshell-enabled photonics-based imaging and therapy of cancer. *Technol. Cancer Res. Treat.* **2004**, *3*, 33–40.
17 Park, J. H.; Gu, L.; von Maltzahn, G.; Ruoslahti, E.; Bhatia, S. N.; Sailor, M. J. Biodegradable luminescent porous silicon nanoparticles for in vivo applications. *Nat. Mater.* **2009**, *8*, 331–336.
18 Godin, B.; Gu, J.; Serda, R. E.; Bhavane, R.; Tasciotti, E.; Chiappini, C.; Liu, X.; Tanaka, T.; Decuzzi, P.; Ferrari, M. Tailoring the degradation kinetics of mesoporous silicon structures through PEGylation. *J. Biomed. Mater. Res. Part A* **2010**, *94*, 1236–1243.
19 Canham, L. T.; INSPEC (Information service). *Properties of porous silicon*; INSPEC: London, 1987.

20 Alvarez, S. D.; Derfus, A. M.; Schwartz, M. P.; Bhatia, S. N.; Sailor, M. J. The compatibility of hepatocytes with chemically modified porous silicon with reference to in vitro biosensors. *Biomaterials* **2009**, *30*, 26–34.

21 Canham, L. T.; Stewart, M. P.; Buriak, J. M.; Reeves, C. L.; Anderson, M.; Squire, E. K.; Allcock, P.; Snow, P. A. Derivatized Porous Silicon Mirrors: Implantable Optical Components with Slow Resorbability. *Phys. Status Solidi A* **2000**, *182*, 521–525.

22 Anglin, E. J.; Cheng, L.; Freeman, W. R.; Sailor, M. J. Porous silicon in drug delivery devices and materials. *Adv. Drug Delivery Rev.* **2008**, *60*, 1266–1277.

23 Tanaka, T.; Mangala, L. S.; Vivas-Mejia, P. E.; Nieves-Alicea, R.; Mann, A. P.; Mora, E.; Han, H. D.; Shahzad, M. M.; Liu, X.; Bhavane, R.; Gu, J.; Fakhoury, J. R.; Chiappini, C.; Lu, C.; Matsuo, K.; Godin, B.; Stone, R. L.; Nick, A. M.; Lopez-Berestein, G.; Sood, A. K.; Ferrari, M. Sustained small interfering RNA delivery by mesoporous silicon particles. *Cancer Res.* **2010**, *70*, 3687–3696.

24 Salonen, J.; Laitinen, L.; Kaukonen, A. M.; Tuura, J.; Bjorkqvist, M.; Heikkila, T.; Vaha-Heikkila, K.; Hirvonen, J.; Lehto, V. P. Mesoporous silicon microparticles for oral drug delivery: loading and release of five model drugs. *J. Controlled Release* **2005**, *108*, 362–374.

25 Sun, W.; Puzas, J. E.; Sheu, T.-J.; Fauchet, P. M. Porous silicon as a cell interface for bone tissue engineering. *Phys. Status Solidi A* **2007**, *204*, 1429–1433.

26 Ananta, J. S.; Godin, B.; Sethi, R.; Moriggi, L.; Liu, X.; Serda, R. E.; Krishnamurthy, R.; Muthupillai, R.; Bolskar, R. D.; Helm, L.; Ferrari, M.; Wilson, L. J.; Decuzzi, P. Geometrical confinement of gadolinium-based contrast agents in nanoporous particles enhances T1 contrast. *Nat. Nanotechnol.* **2010**, *5*, 815–821.

27 Chiappini, C.; Liu, X.; Fakhoury, J. R.; Ferrari, M. Biodegradable Porous Silicon Barcode Nanowires with Defined Geometry. *Adv. Funct. Mater.* **2010**, *20*, 2231–2239.

28 Serda, R. E.; Mack, A.; Pulikkathara, M.; Zaske, A. M.; Chiappini, C.; Fakhoury, J. R.; Webb, D.; Godin, B.; Conyers, J. L.; Liu, X. W.; Bankson, J. A.; Ferrari, M. Cellular association and assembly of a multistage delivery system. *Small* **2010**, *6*, 1329–1340.

29 Serda, R. E.; Mack, A.; van de Ven, A. L.; Ferrati, S.; Dunner, K., Jr.; Godin, B.; Chiappini, C.; Landry, M.; Brousseau, L.; Liu, X.; Bean, A. J.; Ferrari, M. Logic-embedded vectors for intracellular partitioning, endosomal escape, and exocytosis of nanoparticles. *Small* **2010**, *6*, 2691–2700.

30 Serda, R. E.; Ferrati, S.; Godin, B.; Tasciotti, E.; Liu, X.; Ferrari, M. Mitotic trafficking of silicon microparticles. *Nanoscale* **2009**, *1*, 250–259.

31 Tasciotti, E.; Godin, B.; Martinez, J. O.; Chiappini, C.; Bhavane, R.; Liu, X.; Ferrari, M. Near-infrared imaging method for the in vivo assessment of the biodistribution of nanoporous silicon particles. *Mol. Imaging* **2011**, *10*, 56–68.

32 Decuzzi, P.; Godin, B.; Tanaka, T.; Lee, S. Y.; Chiappini, C.; Liu, X.; Ferrari, M. Size and shape effects in the biodistribution of intravascularly injected particles. *J. Controlled Release* **2010**, *141*, 320–327.

33 Fire, A.; Xu, S.; Montgomery, M. K.; Kostas, S. A.; Driver, S. E.; Mello, C. C. Potent and specific genetic interference by double-stranded RNA in Caenorhabditis elegans. *Nature* **1998**, *391*, 806–811.

34 Davis, M. E.; Zuckerman, J. E.; Choi, C. H.; Seligson, D.; Tolcher, A.; Alabi, C. A.; Yen, Y.; Heidel, J. D.; Ribas, A. Evidence of RNAi in humans from systemically administered siRNA via targeted nanoparticles. *Nature* **2010**, *464*, 1067–1070.

35 Mangala, L. S.; Han, H. D.; Lopez-Berestein, G.; Sood, A. K. Liposomal siRNA for ovarian cancer. *Methods Mol. Biol.* **2009**, *555*, 29–42.

36 Whitehead, K. A.; Langer, R.; Anderson, D. G. Knocking down barriers: advances in siRNA delivery. *Nat. Rev. Drug Discovery* **2009**, *8*, 129–138.